CFD Model Development of a Cryogenic Storage Tank Self-Pressurization in Normal Gravity and Validation against SHIIVER Experiment

Olga Kartuzova[1] and Mohammad Kassemi[2]
National Center for Space Exploration Research (NCSER), Case Western Reserve University and NASA Glenn Research Center, Cleveland, OH 44135, USA
Daniel Hauser[3]
NASA Glenn Research Center, Cleveland, OH 44135, USA

Two-phase flow and heat transfer simulations with interfacial phase change of the Structural Heat Intercept, Insulation, and Vibration Evaluation Rig (SHIIVER) self-pressurization experiment were conducted using storage tank CFD model in the framework of the ANSYS Fluent CFD code. The simulations were performed for the 70% fill level case with MLI on domes and no vapor cooling. All the phase change calculations in these simulations were generated by in-house Schrage-based evaporation-condensation model. The calculations were performed using both the Volume of Fluid (VOF) and Sharp Interface multiphase 2D axisymmetric models. A number of parametric and sensitivity studies were performed to check the various aspects of the CFD model. These studies helped to understand the effects of varying several parameters on the tank pressure and temperature during self-pressurization. Turbulence modeling; turbulence damping at the interface; and using constant vs. temperature dependent fluid properties were shown to have the most profound influence on predicted tank pressures and temperatures. Current study indicates that including phase change at the interface into the computational model is crucial for accurate prediction of the tank self-pressurization process. The effect of accommodation coefficient was also studied. Tank pressure values predicted by the VOF, and Sharp Interface models are within 4% of the experimental ones.

I. Nomenclature

E	=	energy, J
F	=	force, N
g	=	gravitational acceleration, m/s^2
h	=	enthalpy, J/kg
k	=	thermal conductivity, W/m·K
$\boldsymbol{n}$	=	normal vector
p, P	=	pressure, Pa
t	=	time, seconds
T	=	temperature, K
v	=	velocity, m/s
Greek		
α	=	cell value of volume fraction
μ	=	Pa·s
ρ	=	density, kg/m^3
σ	=	surface tension, N/m

[1] Research Assistant Professor, Department of Mechanical & Aerospace Engineering, and AIAA Member.
[2] Research Professor, Department of Mechanical & Aerospace Engineering, AIAA Associate Fellow.
[3] Fluids Engineer, Fluid and Cryogenic Systems Branch.

Subscripts
eff = effective
i = interface
q = phase

II. Introduction

The Structural Heat Intercept, Insulation, and Vibration Evaluation Rig (SHIIVER) is a large-scale cryogenic fluid management (CFM) test bed designed to scale CFM technologies for inclusion on large, in-space stages[1]. A part of the NASA evolvable Cryogenics (eCryo) project, SHIIVER is a technology development task that is supportive of future exploration propulsion needs. This experiment also provided valuable data for assessing the ability of the currently available computational models to accurately predict self-pressurization of a cryogenic storage tank in 1g.

A number of computational models with different degrees of sophistication have been developed to study storage tank operations in 1g and/or microgravity[2]. Many of these models provided validations against tank self-pressurization[3-6] experiments. Kassemi et al.[7] provided a review of different computational approaches to modeling cryogenic tank self-pressurization. They developed sharp and diffused interface computational models utilizing kinetics formulation for near equilibrium conditions to calculate phase change. These models were applied to model three different tank self-pressurization experiments, two with simulant fluid in 1g and microgravity and one with LH2 in 1g, with great success. However, a comprehensive review of the effects of different numerical parameters on computational results is desirable. This is the goal of the current paper.

In the two-phase CFD model of the SHIIVER test tank presented in this paper, two computational approaches to modeling liquid-vapor interface are compared. These are the Volume-of-Fluid (VOF) and the Sharp Interface techniques. Both methods use a kinetic-based mass transfer submodel to evaluate the evaporative-condensing interfacial mass transfer. In this type of model an accommodation coefficient is used to represent an evaporation or condensation ratio at the interface. The value of the accommodation coefficient can vary between 0 and 1. The values of the accommodation coefficient for a water-air interface have been extensively studied in the literature. A comprehensive review of research on the water Accommodation Coefficient (AC) is presented by Marek and Straub[8]. However, there is very little information in the literature on the values of the accommodation coefficient for hydrogen. Kartuzova and Kassemi[9] studied effect of AC on the hydrogen filled tank pressure rise during tank self-pressurization. However, in their study the tank was subjected to a very low heat flux (0.9 W/m^2 in the vapor and 2 W/m^2 in the liquid). An effect of the accommodation coefficient used for calculating the interfacial mass transfer rate on the tank pressure rise during tank self-pressurization is analyzed in this study for a tank with more realistic heat loads, where local heat flux could reach 200-300 W/m^2.

The objective of the present study is to assess the ability of the current CFD model to accurately predict self-pressurization of a cryogenic storage tank in normal gravity by comparing CFD results with the tank pressure and temperature data provided by the SHIIVER experiments. Effects of turbulence modeling in the bulk fluid and at the interface; fluid properties (constant vs. temperature dependent); accommodation coefficient; and phase change are studied. The results of the Sharp Interface and the VOF methods are compared with each other and with the experimental data.

III.Experimental setup

In the experiment a 4 m internal diameter, 3.3 m tall tank known as the Structural Heat Intercept, Insulation, and Vibration Evaluation Rig (SHIIVER) was used. SHIIVER was configured with structural skirts and fluid lines similar to a launch vehicle upper stage arrangement. The performance goals of the SHIIVER testing involve demonstrating the improved performance (through reduced boil-off) provided to a large-scale liquid hydrogen tank by applying MLI and vapor cooling of skirts[1].

IV. Mathematical Model

A. Governing Equations

Fluid flow and heat transfer in the tank are described in terms of the continuity, Navier-Stokes and energy equations for both phases:

$$\frac{\partial \rho}{\partial t} + \nabla(\rho \mathbf{v}) = 0, \tag{1}$$

$$\frac{\partial}{\partial t}(\rho \mathbf{v}) + \nabla(\rho \mathbf{v}\mathbf{v}) = -\nabla p + \nabla\left[\mu_{eff}(\nabla \mathbf{v} + \nabla v^T)\right] + \rho \mathbf{g} + \mathbf{F}_{vol}, \tag{2}$$

$$\frac{\partial}{\partial t}(\rho E) + \nabla\big(\mathbf{v}(\rho E + p)\big) = \nabla\big(k_{eff}\nabla T\big) + S_h. \tag{3}$$

In the present study, the liquid phase is treated as incompressible with variable temperature-dependent properties, except for density. The liquid density is allowed to vary linearly with temperature in the body force term of the momentum equation according to the Boussinesq approximation. The vapor is modeled as a compressible ideal gas. In this study, the movement of the interface is captured diffusely using the Volume of Fluid (VOF) method, as promogulated by Hirt and Nichols[10]. Interfacial energy, momentum and mass balances are applied using source terms in the diffuse interfacial region.

B. VOF Model

In the VOF method, a volume fraction is defined in each cell such that the volume fractions of all the phases sum to unity. In the cell, the change in the interface can be tracked by solving a continuity equation for the volume fraction of the q^{th} phase:

$$\frac{1}{\rho_q}\left[\frac{\partial}{\partial t}(\alpha_q \rho_q) + \nabla \cdot (\alpha_q \rho_q \mathbf{v}_q) = S_{\alpha_q}\right], \tag{4}$$

where the volume fraction for the primary phase is determined from:

$$\sum_{q=1}^{n} \alpha_q = 1. \tag{5}$$

In the VOF method, the field variables and properties are defined in terms of the volume fraction, which for a general system can be written as:

$$\rho = \sum_{q=1}^{n} \alpha_q \rho_q, \qquad \mu_{eff} = \sum_{q=1}^{n} \alpha_q \mu_{eff_q}, \qquad k_{eff} = \sum_{q=1}^{n} \alpha_q k_{eff_q}. \tag{6}$$

In this fashion, the continuity, momentum and energy equations, as described by Eq. (1) – (3), can be solved throughout the domain for the temperatures and velocities in the two phases. In the VOF model, energy (E) and temperature (T) are treated as mass-averaged variables:

$$E = \frac{\sum_{q=1}^{n} \alpha_q \rho_q E_q}{\sum_{q=1}^{n} \alpha_q \rho_q}, \tag{7}$$

where E_q is based on the specific heat of the q^{th} phase and the shared temperature.

Evaporation and condensation at the interface are modeled as a source term in the continuity equation for the volume fraction (Eq. 4), i.e.:

$$S_{\alpha_q} = \dot{\mathbf{m}}_i \cdot \mathbf{A}_i\,, \tag{8}$$

where $\mathbf{A}_i$ is an interfacial area density vector, and $\dot{\mathbf{m}}_i$ is a mass flux vector, which for near equilibrium conditions can be determined based on the Schrage[3] equation:

$$|\dot{\mathbf{m}}| = \left(\frac{2\sigma}{2-\sigma}\right)\left(\frac{M}{2\pi R}\right)^{1/2}\left(\frac{P_i}{T_i^{1/2}} - \frac{P_v}{T_v^{1/2}}\right). \tag{9}$$

Here σ is the accommodation coefficient; M is the molar mass of the fluid; R is the universal gas constant; P_i and P_v are, respectively, the interfacial and vapor pressures (it was assumed that $P_i \cong P_{sat}$); T_i and T_v are, respectively, the interfacial and vapor temperatures (it was assumed that $T_i = T_v \cong T_{sat}$ at the interface). Finally, $\mathbf{A}_\mathbf{i}$ is defined as:

$$\mathbf{A}_i = |\nabla \alpha|, \tag{10}$$

where α is the volume fraction of the primary phase.

In the present implementation, the surface tension forces at the interface are modeled via the Continuum Surface Force (CSF) model of Brackbill et al.[12]. In this model, the surface tension forces at the interface are transformed into a volume force ($\mathbf{F}_{vol}$), which is added as a source to the momentum equation:

$$\mathbf{F}_{vol} = \sum_{pairs\ ij, i<j} \sigma_{ij} \frac{\alpha_i \rho_i h_i \nabla \alpha_j + \alpha_j \rho_j h_j \nabla \alpha_i}{\frac{1}{2}(\rho_i + \rho_j)}\,, \tag{11}$$

where h_i is the surface curvature calculated from the local gradients in the surface normal at the interface:

$$h_i = \nabla \cdot \hat{\mathbf{n}}. \tag{12}$$

C. Sharp Interface Model

In the Sharp Interface model, the governing equations are solved separately for the liquid and vapor domains. The two phases are coupled at the interface through the continuity of velocities and shear stresses, as well as an energy balance performed at the interface boundary:

$$\left|\dot{\mathbf{m}}\right| L = \mathbf{q}_{il} - \mathbf{q}_{iv} . \tag{13}$$

Here $\left|\dot{\mathbf{m}}\right|$ is an interfacial mass transfer rate determined from the previously defined Schrage equation (Eq. 9); $\mathbf{q}_{il}$ and $\mathbf{q}_{iv}$ are conductive heat fluxes on the liquid and vapor sides of the interface:

$$\mathbf{q}_{il} = -k_{l\_eff} \nabla T \,|_l \tag{14}$$

$$\mathbf{q}_{iv} = -k_{v\_eff} \nabla T \,|_v \tag{15}$$

In this approach, the interfacial temperature is determined from (13) and essentially approaches saturation temperature only when mass transfer is small, i.e. at near equilibrium conditions.

In order to ensure velocity continuity at the interface, the tangential velocity component on the vapor side of the interface is set equal to the one from the liquid side:

$$v_{\tan g\_v} = v_{\tan g\_l} , \tag{16}$$

and the tangential component of the interfacial shear stress from the vapor side is applied to the liquid side of the interface:

$$\tau_{\tan g\_l} = \tau_{\tan g\_v} \tag{17}$$

D. Turbulence Modeling

In this study, the tank turbulence was modeled by utilizing the Shear Stress Transport k-ω model of Menter[13] (kw-SST). This model is similar to the standard k-ω model of Wilcox,[14] but has the ability to account for the transport of the principal shear stress in adverse pressure gradient boundary layers. These features make the kw-SST model more accurate and reliable for a wider class of flows than the standard k-ω model.

In the VOF model, continuity of the turbulent quantities is inherently assumed since one set of equations for the turbulent kinetic energy and dissipation rate is solved for both phases throughout the domain, with properties varying according to the local volume fraction value.

V. Numerical Implementation

A. Tank Geometry

Tank geometry, which consists of fluid inside the tank and the tank wall, used in CFD calculations is shown in Fig. 1.

B. Initial Conditions

Initial tank pressure was set to the measured value of 20 psia (137,895.1 Pa). Measured fluid temperatures before the beginning of self-pressurization test were used to obtain initial temperature conditions for CFD runs. Initial fill level value of 66.37% was used. In the cases where turbulence models were used initial values for turbulence kinetic energy and specific dissipation rate were set, respectively, to 1 x10^{-6}, m^2/s^2 and 100, 1/s.

C. Boundary Conditions

The tank wall was included in calculations. Heat fluxes on the outside of the tank wall which considered heat transfer in the forward and aft skirts and MLI insulation on the domes were calculated in a separate Thermal Desktop Model and applied as boundary conditions in CFD, as shown in Fig. 2. Preliminary estimates of the heat loads were used here. Lower values of the heat flux on the domes were later published in the experimental report[1], however since most heat is entering the tank through the barrel (not covered by MLI) and flanges (conducting heat from the attached skirts) this discrepancy is unlikely to significantly affect the results. A contact angle between the liquid and tank wall was assumed to be 0 degrees. No slip boundary conditions were applied on the inside of the tank wall which was in contact with fluid.

D. Material Properties

The liquid hydrogen and its vapor filled the tank in the experiment. Constant material properties were used for the working fluid, except for C_p, thermal conductivity and viscosity, which were temperature dependent in a pricewise-linear fashion. The properties are summarized in Table 1.

The tank wall material, stainless steel was modeled with temperature dependent C_p and thermal conductivity and constant density equal to 7700 kg/m^3.

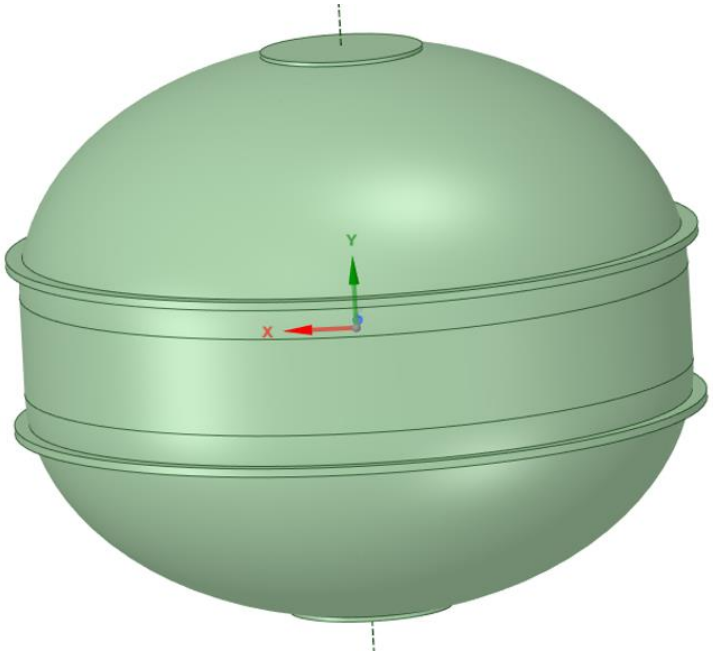

Figure 1: SHIIVER tank geometry used for calculations

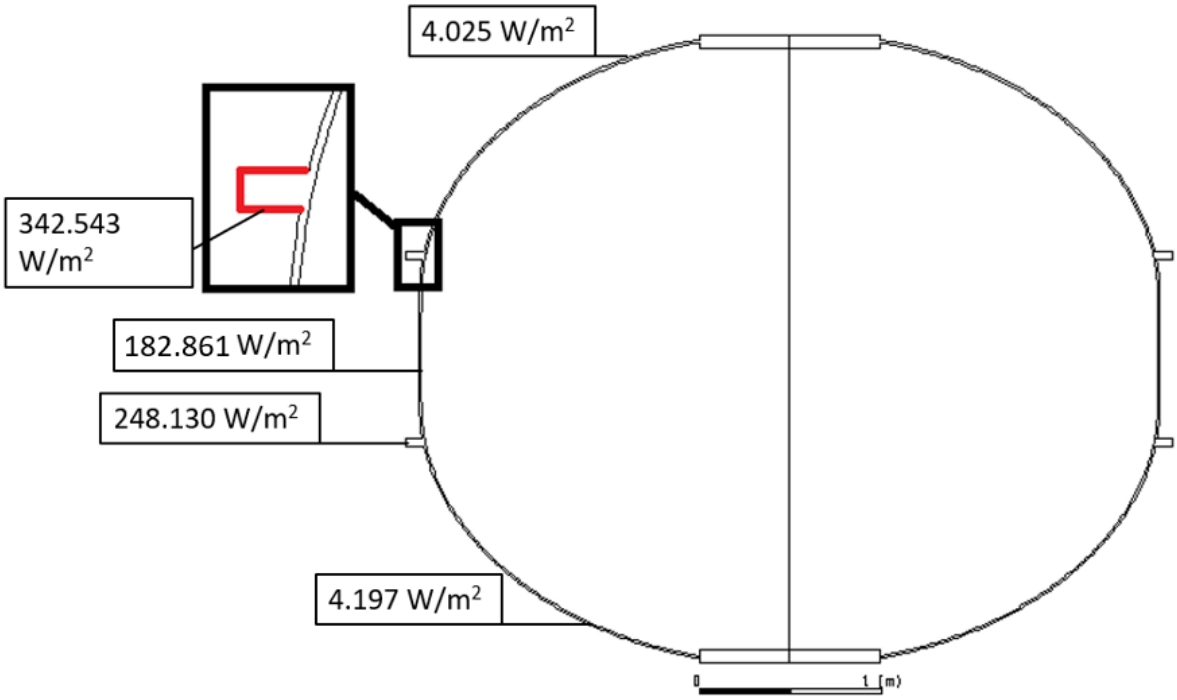

Figure 2: Heat fluxes applied in Fluent as B.C.

Table 1. Parahydrogen properties from NIST:

Property	Units	liquid	vapor
Density	kg/m^3	69.544	Ideal gas
C_p	J/kg-K	func(T)	func(T)
Thermal Conductivity	W/m-K	func(T)	func(T)
Viscosity	Pa*s	func(T)	func(T)
Surface Tension	N/m	0.0017502	
Thermal Expansion coeff.	1/K	0.0168	-
Molecular Weight	kg/kmol	2.0159	

E. Computational Mesh

Four different 2D axisymmetric computational grids were used in the current study. Their characteristics are summarized in Table 2. The refinement 2 mesh is shown in Fig. 3. A grid independence study was conducted, and the results are presented in the "results and discussion" section of this paper.

Table 2. Mesh Characteristics

Name	Refinement 0 (Coarse)	Refinement 1	Refinement 2	Refinement 3
First cell at	5 mm	1 mm	0.5 mm	0.1 mm
Number of cells	43,744	45,538	96,559	98,623

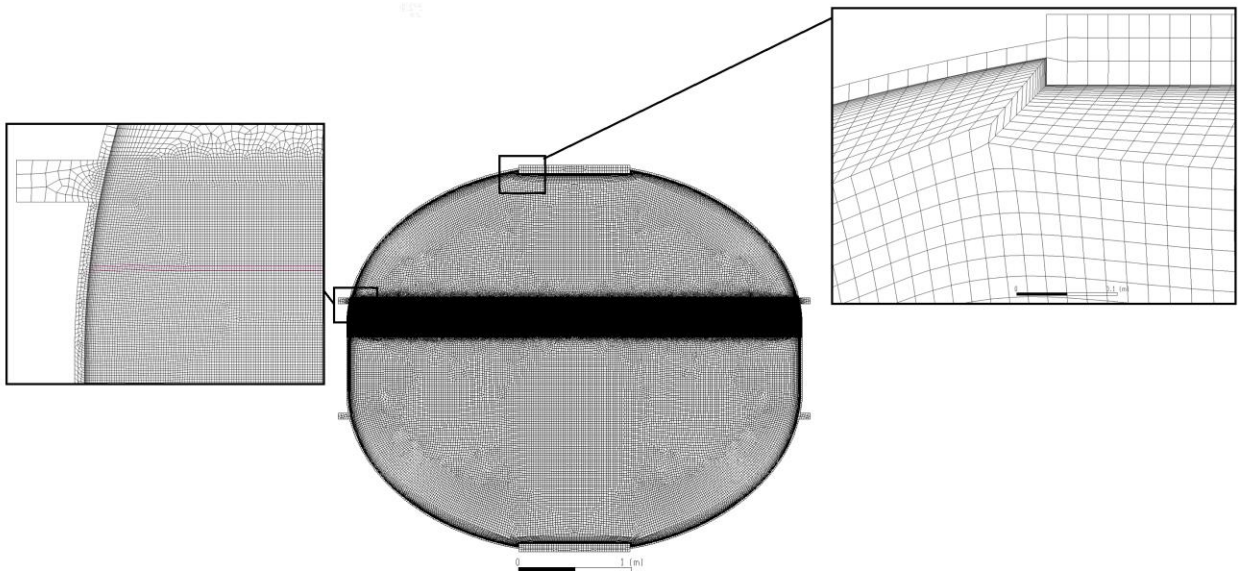

Figure 3: Computational Mesh – Refinement 2 (96,559 cells)

F. Discretization and Convergence

The Second Order Upwind scheme was used to discretize the turbulence, energy, and momentum equations (cell values). The PISO scheme was used for the pressure-velocity coupling (cell values). The Least Squares Cell Based scheme was used for the gradient calculations (face values). The PRESTO! scheme was used for the pressure interpolation (face values). The Point Implicit (Gauss-Seidel) linear equation solver with the Algebraic Multi-Grid (AMG) method was used to solve the linearized systems of equations. The First Order Implicit temporal discretization scheme was used with the explicit VOF model. The Geometric Reconstruction scheme was used to discretize the VOF

equation. The convergence criteria are set to $1x10^{-4}$ for all the equations except the energy equation, for which it is set to $1x10^{-6}$. Time step size independence study was conducted, based on the results of this study a value of 0.01 seconds was selected.

VI. Results and Discussion

The SHIIVER case with 70% fill level, MLI on domes and no vapor cooling was modeled using 2D axisymmetric formulation.

A. Grid Independence Study

Grid Independence was tested using four different meshes. The details of these meshes are summarized in Table 2. The results of the grid independence test are presented in Fig. 4 in a form of tank pressure evolution comparison between different grids and with the experimental data. As shown in Fig. 4, all meshes result in similar tank pressure values, except for the coarsest mesh which significantly under-predicts the tank pressures. The mesh with Refinement 2 was selected for this study. This decision is based on the tank pressure and velocity field near the tank wall predicted by this mesh.

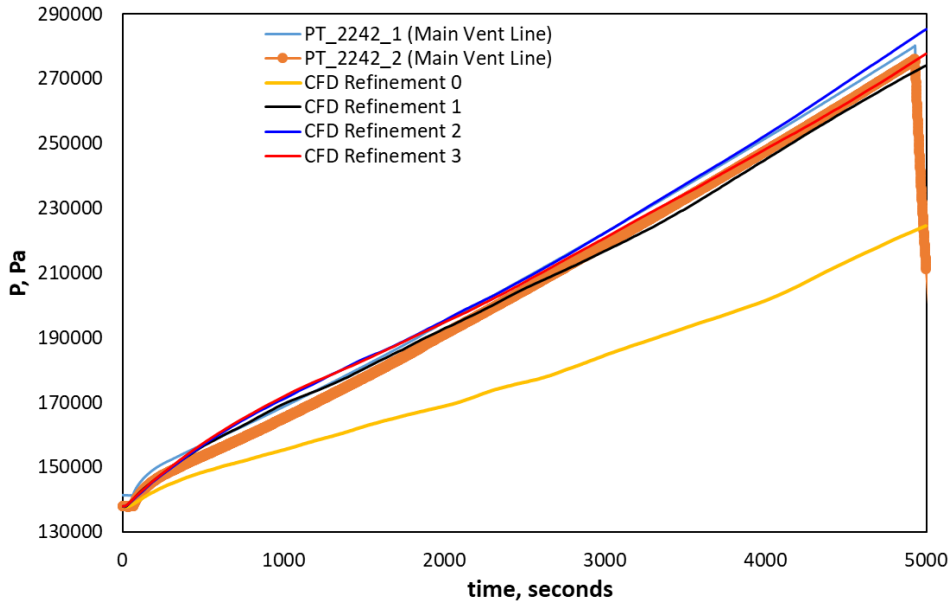

Figure 4: Grid Independence Study

B. Time Step Size Sensitivity Study

Three different time step sizes were tested in this study. Resulting tank pressure evolutions are compared with the experimental data in Fig. 5. The two lower time step sizes tested (0.001s and 0.01s) result in similar tank pressures. The highest time step size of 0.02 s resulted in higher than experimental tank pressures and faster tank pressure rise towards the end of simulation. The time step size value of 0.01s was selected for this study.

C. The Effect of Turbulence Modeling: Laminar vs. Turbulent

The effect of turbulence modeling was evaluated using Laminar (no Turbulence model used) and Turbulent (k-w-SST) models. Tank pressures predicted by these two models are compared with the experimental data in Fig. 6. The Laminar model results in tank pressures which match experimental data very well. The Turbulent model significantly underpredicts tank pressures compared to the experimental data.

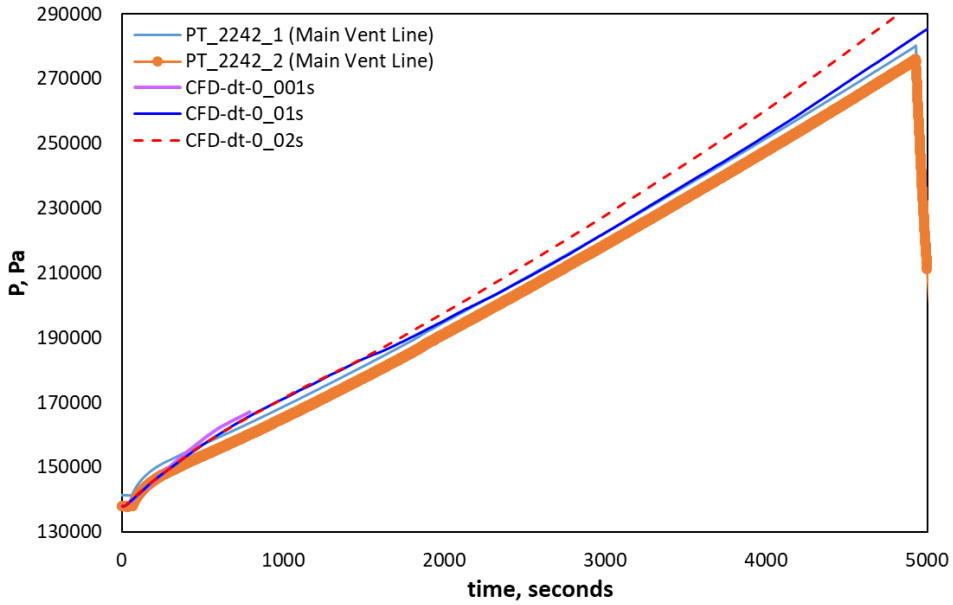

Figure 5: Time step size sensitivity study

D. The Effect of Turbulence Damping at the Interface

When the VOF model is used together with the turbulence model continuity of turbulent quantities at the interface is applied due to the nature of the VOF model. This creates high levels of turbulence at the interface which affects interfacial heat and mass transfer, and, in turn, tank pressures, predicted by the Turbulent VOF model. There is an option in ANSYS Fluent to use turbulence damping at the interface with the Turbulent VOF model. The effect of turbulence damping at the interface on the tank pressure was studied and the results of the models without damping and with damping coefficient of a 100 are presented and compared with the experimental pressures in Fig. 7. The results of the Laminar model are also shown in Fig. 7 for reference. Even though the turbulent model with turbulent damping at the interface did improve the results over the turbulent model without damping, it still significantly underpredicted experimentally measured tank pressures.

E. The Effect of Temperature Dependent Fluid Properties

The effect of fluid properties used in the simulation was studied. All constant fluid properties (at the initial tank saturation conditions) are compared with temperature dependent Cp, k and μ for both liquid and vapor. Tank pressures predicted by the models are presented in Fig. 8. The model with constant properties results in higher tank pressures and faster pressure rise compared to the model with variable properties. The model with temperature dependent properties predicts both the slope and values of the tank pressure that match the experimental ones closely.

F. The Effect of Accommodation Coefficient

Since the Schrage equation utilized to predict mass transfer rate at the interface relies on the value of accommodation coefficient used, its effect needs to be studied. The Schrage equation is designed to predict phase change rate at the interface at near equilibrium conditions. Tank self-pressurization is a slow process which doesn't deviate much from equilibrium; therefore, the Schrage equation is applicable, and the results should be independent from the value of accommodation coefficient. The effect of accommodation coefficient on tank pressure was studied and the results are shown in Figure 9, where two values of accommodation coefficient are compared. Those values are 0.001 and 0.01. The figure indicates that, as it was expected, the effect of accommodation coefficient on tank pressure is negligible. A higher value of accommodation coefficient should result in similar results, however, as shown by Kartuzova and Kassemi,[10] using higher than 0.01 accommodation coefficients with the VOF model results in numerical instabilities and requires smaller time step sizes, therefore it hasn't been tested in this study.

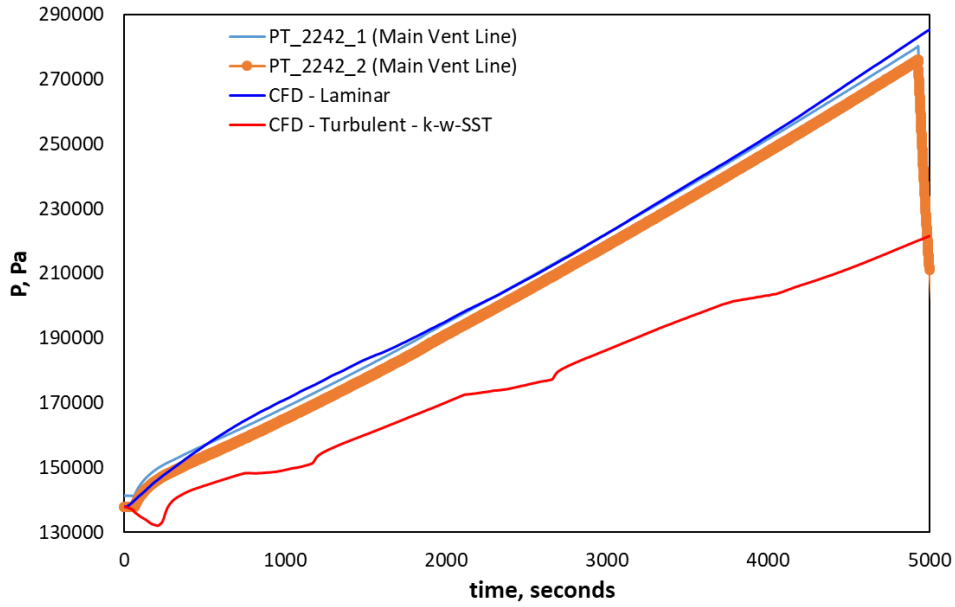

Figure 6: Effect of turbulence modeling – Laminar vs. Turbulent (k-w-SST): Tank Pressure

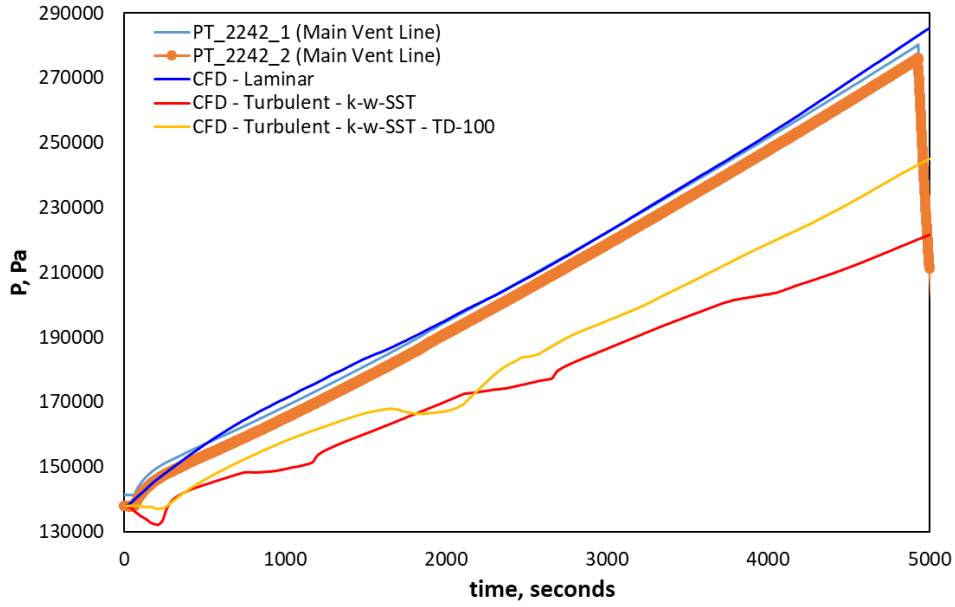

Figure 7: Effect of turbulence damping at the interface: Tank Pressure

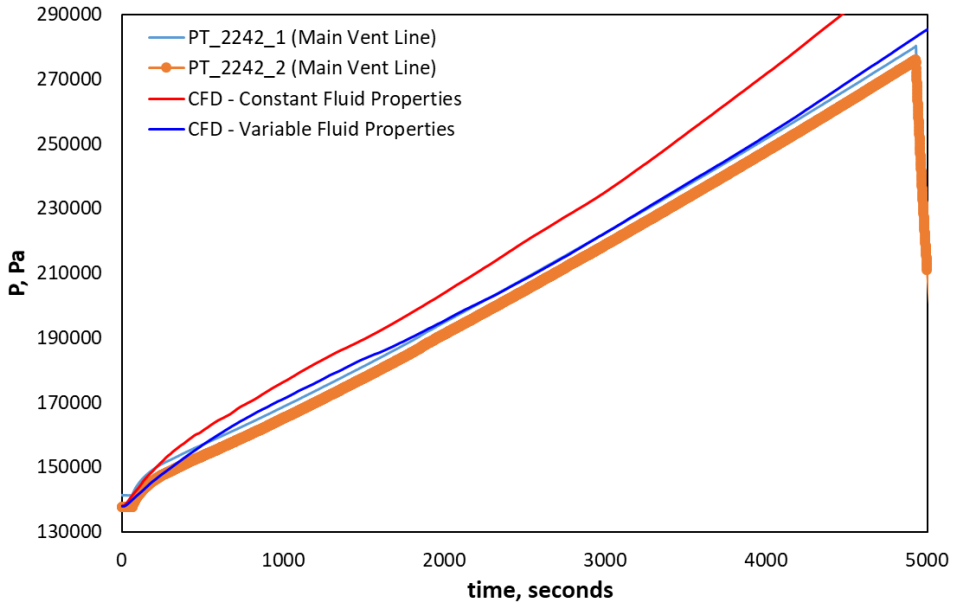

Figure 8: Effect of fluid properties: Tank Pressure

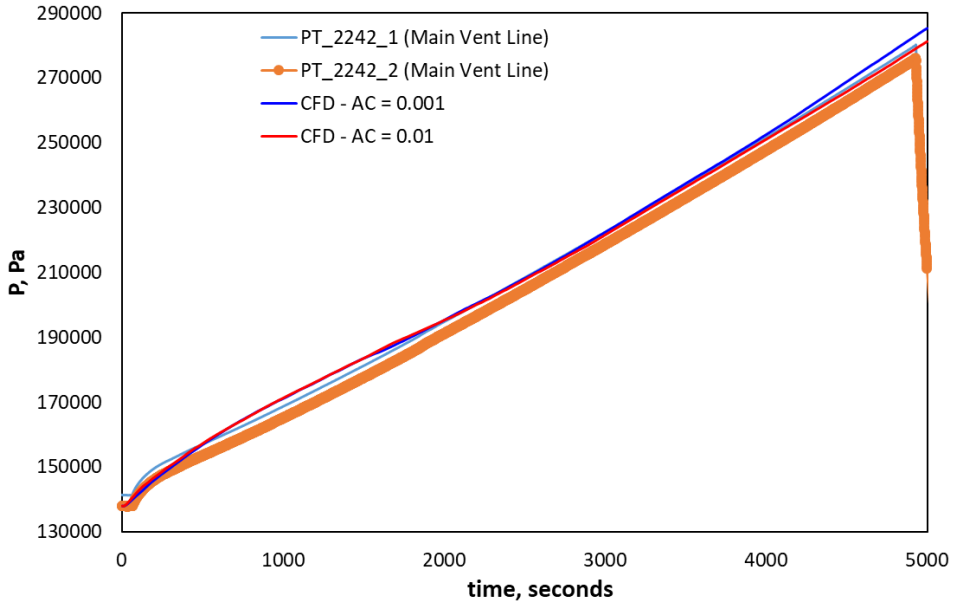

Figure 9: Effect of Accommodation Coefficient: Tank Pressure

G. The Effect of Phase Change at the Interface

In order to study the importance of phase change at the interface in this case and its effect on the tank pressure rise, simulations without phase change were completed and resulting tank pressures predicted by both Laminar and Turbulent models with and without phase change are shown in Figure 10. The results of the CFD models are compared with the measured tank pressures. The results of the Laminar model with phase change match the experimental pressures very well. The Laminar model without phase change significantly underpredicts tank pressures. The Turbulence model with phase change predicts lower tank pressures than in the experiment, however, it results in higher tank pressures than the Laminar model without phase change. The Turbulent simulation without phase change predicts the lowest tank pressures among all models. It predicts initial pressure drop and then almost constant pressure for the

rest of the run. These results show that the phase change is an important mechanism for rising tank pressure in this self-pressurization case. In the case with the Turbulence model all the pressure rise in the tank is due to phase change.

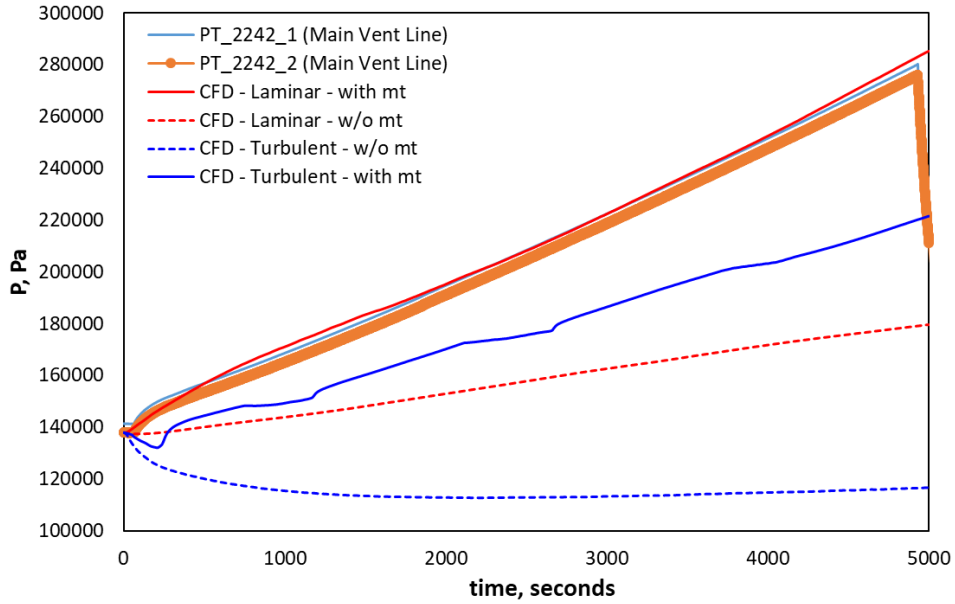

Figure 10: Effect of modeling mass transfer at the interface: Tank Pressure

H. The VOF and Sharp Interface Models Results

Tank pressures predicted using the VOF model are compared with the results of the Sharp Interface model and experiemntal data in Fig. 11. Both models are in a good agreement with the experimental tank pressure values and pressure rise rates. As shown in Fig. 12, differences between the experimental and predicted tank pressures are within 4% for both the Sharp Interface and VOF models. Figure 13 shows comparison between predicted and measured pressure rise rates. The Sharp Interface model underpredicts pressure values and pressure rise rate in the first 1000 seconds, however, it matches the experimental pressure rise rate and the one predicted by the VOF model for the rest of the self-pressurization. Pressure values predicted by this model between 1000 and 5000 seconds match the experimental results very closely. The VOF model matches experiemntal pressure values more closely during the first 300 seconds and slightly over-predicts experimental pressures for the rest of the run. This model predicts an increase in the pressure rise rate during the first 300 seconds and almost constant rate for the rest of the run matching the experimental trend.

Interfacial mass transfer rates predicted by the Sharp Interface and VOF models are shown in Fig. 14. The mass transfer rate predicted by the Sharp Interface model on average matches the one predicted by the VOF model for the most of the run, except initially the Sharp Interface model predicts lower evaporation rates at the interface compared to the results of the VOF model. This is the reason for the lower initial pressure rise predicted by the Sharp Interface model.

Fluid temperatures predicted by the Sharp Interface model are shown in Fig. 15-a. The Fig. 15-b shows comparison of the temperature at the top of the vapor region at the SD83 location predicted by the Sharp Interface and VOF models and compared with the extramental data. Both models predict very similar temperatures in the vapor which are lower than the ones measured in the experiment. Temperature contours at the center plane of the tank at the end of self-pressurization predicted by the Sharp Interface and VOF models are presented in Fig. 16. Temperature ranges for both liquid and vapor regions are shown. Both models result in very similar temperature distributions in the liquid and vapor regions at the end of self pressurization.

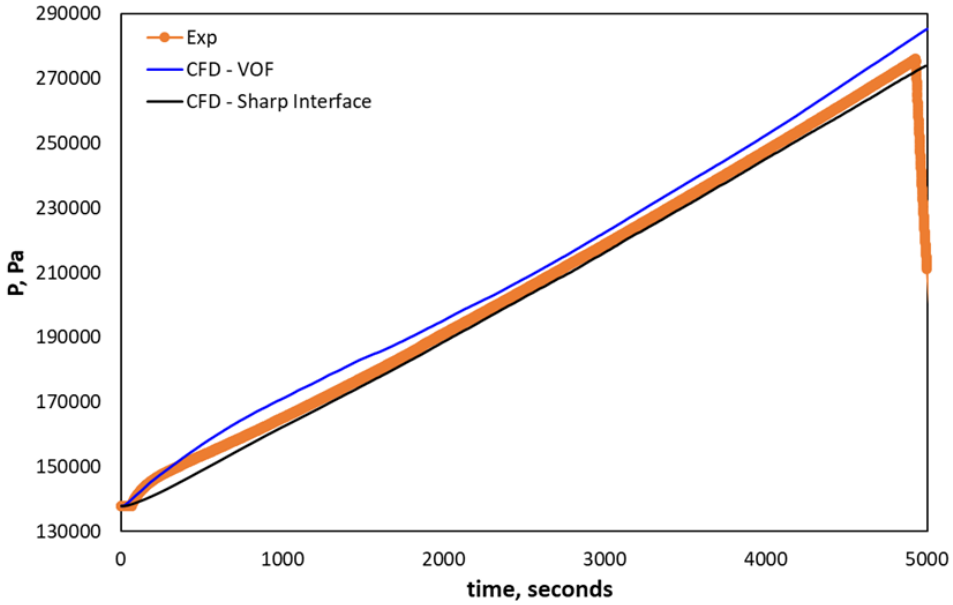

Figure 11: Tank Pressure

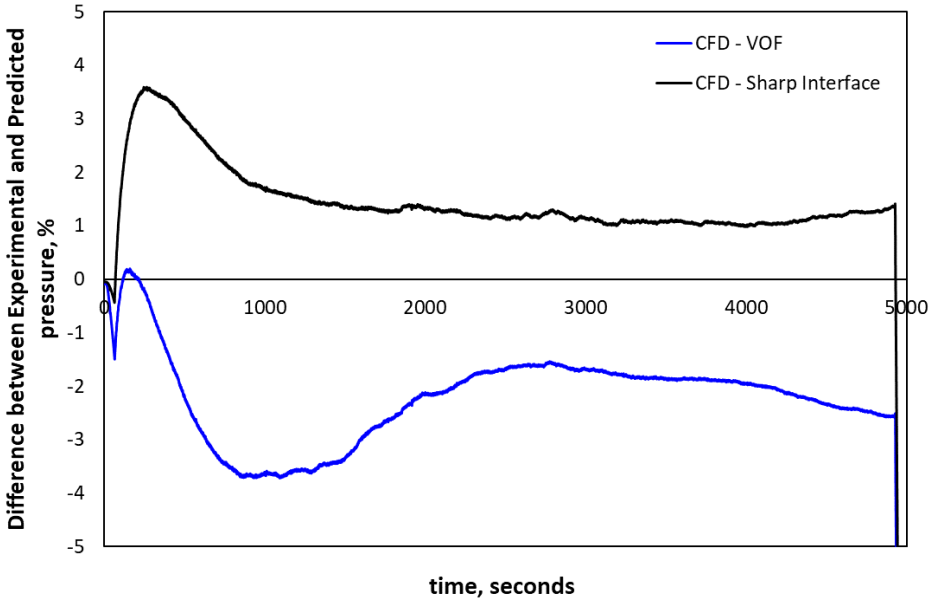

Figure 12 Difference between experimental and predicted tank pressures (in %)

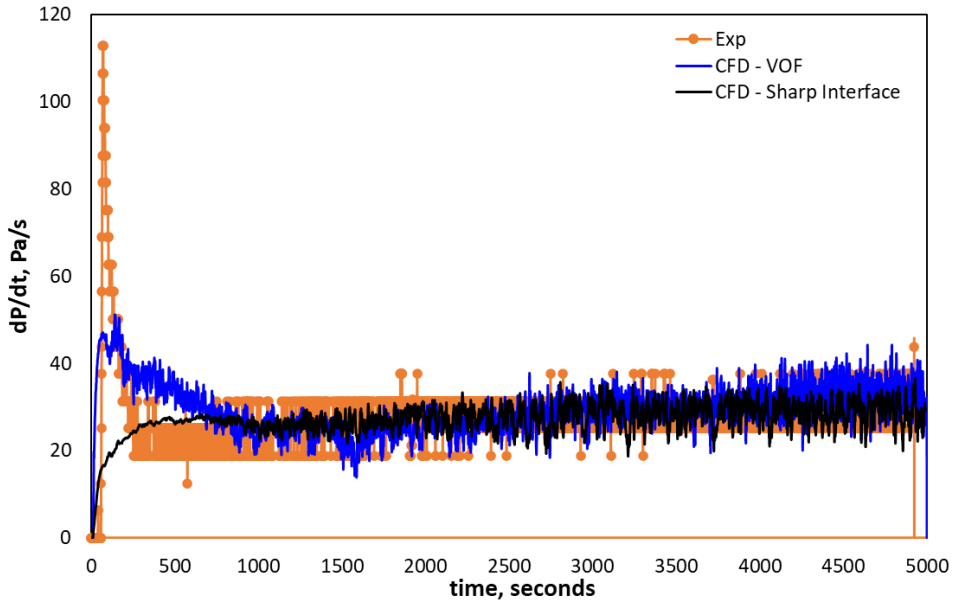

Figure 13 Predicted and experimental pressure rise rates

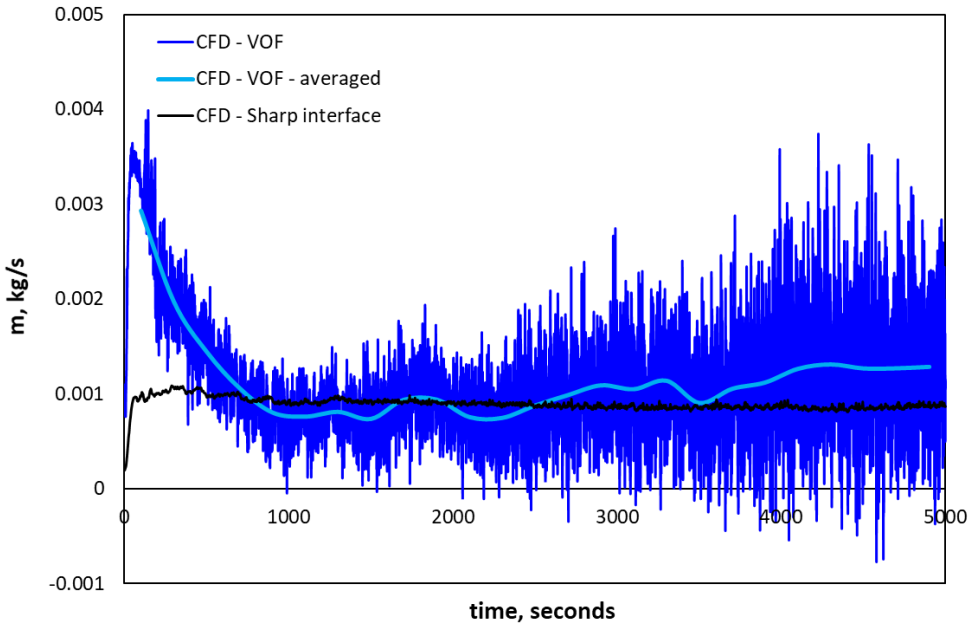

Figure 14: Interfacial Mass Transfer Rate

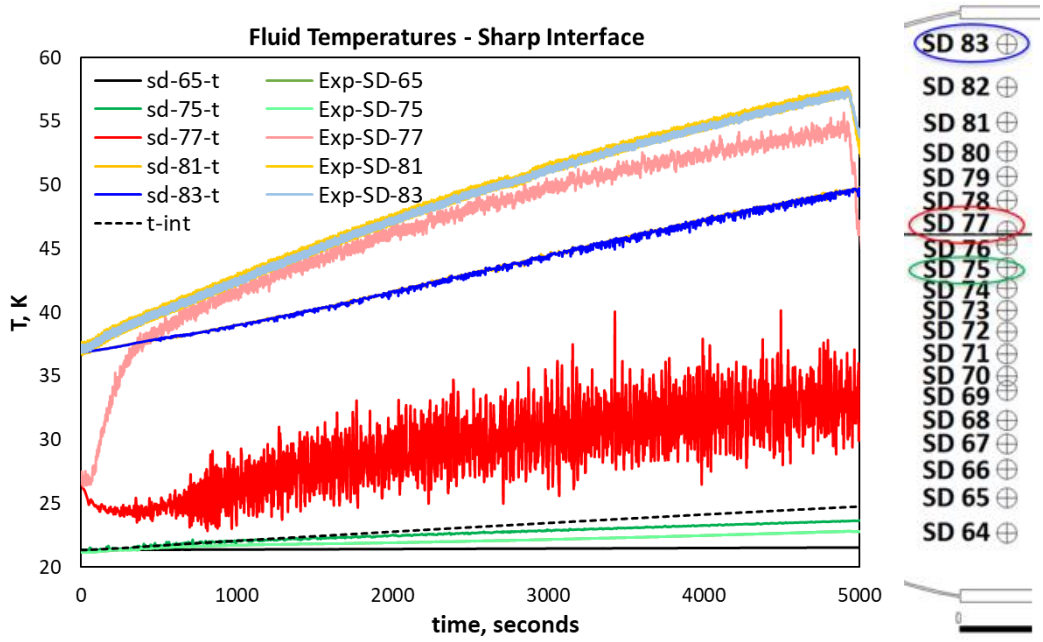

a) Sharp Interface

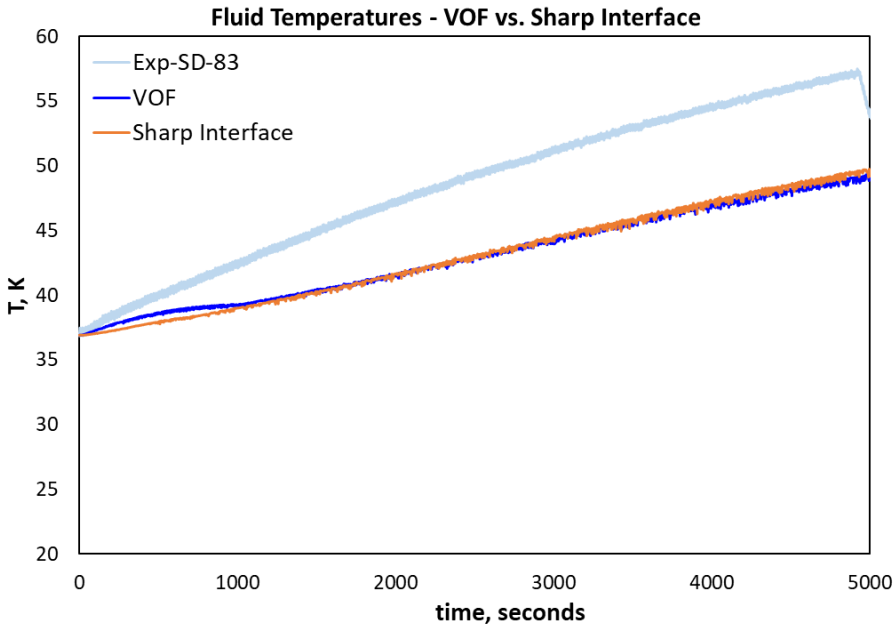

b) Comparison of vapor temperatures at the SD-83 location

Figure 15: Effect of Multiphase Model – Sharp Interface vs. VOF – Fluid Temperatures

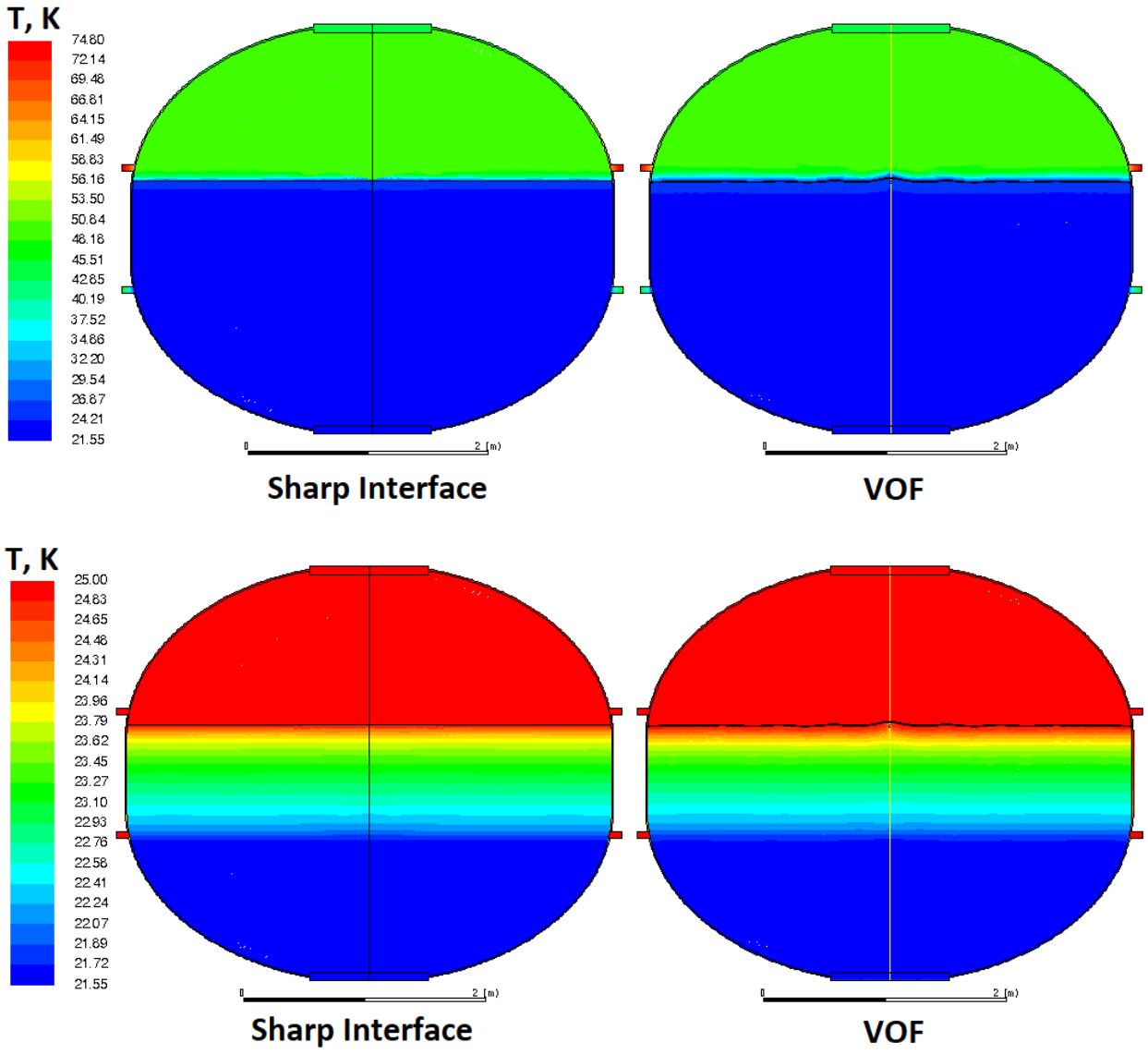

Figure 16: Effect of Multiphase Model – Sharp Interface vs. VOF – Fluid Temperature Contours at 5000 s

I. The Effect of the Tank Heat Load

The effect of the tank heat load was studied with the Sharp Interface multiphase model. Two additional cases were considered. In the first case the heat load for the forward dome was increased from 71 W to 300 W. In the second case the heat load for most of the forward dome was kept the same, except for the flat portion at the top where it was increased to match the barrel heat flux (182 W/m^2). The second case was set up in an attempt to mimic heat entering through structural heat paths in the region at the top of the tank. The results in a form of tank pressure, interfacial mass transfer rate and vapor temperature at the SD83 location are presented in Figs. 17-19 respectively. Tank pressure and temperature at the SD83 location at the top of the vapor region are compared with the experimental data. The results show that increasing the heat load for the top dome doesn't increase the tank pressure much but improves the agreement between the measured and predicted temperatures at the top of the vapor region significantly. The results of the case with the increased heat load for the top flat portion of the tank wall show that the tank pressure and interfacial mass transfer rate are unaffected, but the vapor temperature is slightly improved.

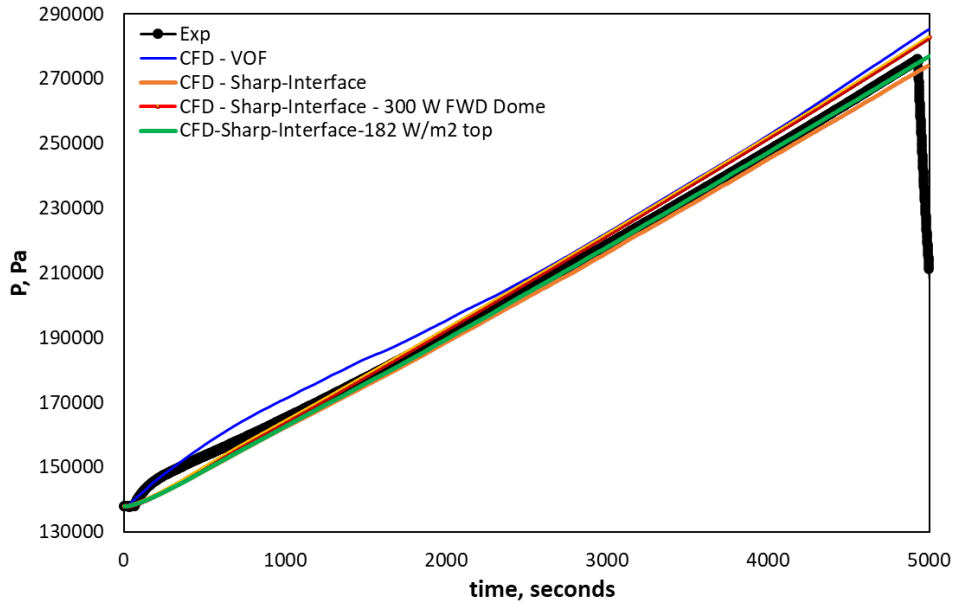

Figure 17: Effect of Tank Heat Load – Tank Pressure

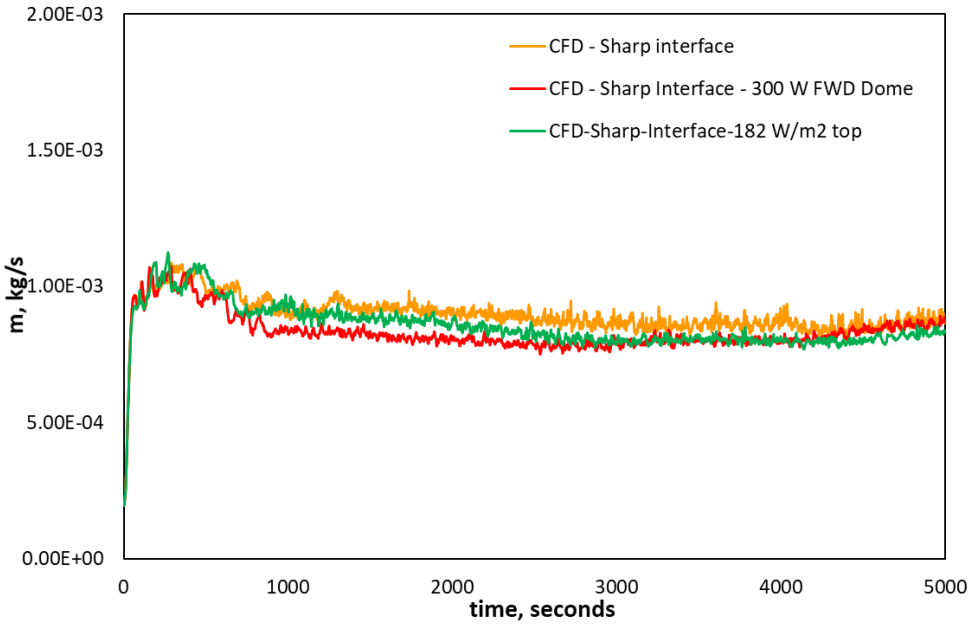

Figure 18: Effect of Tank Heat Load – Interfacial Mass Transfer Rate

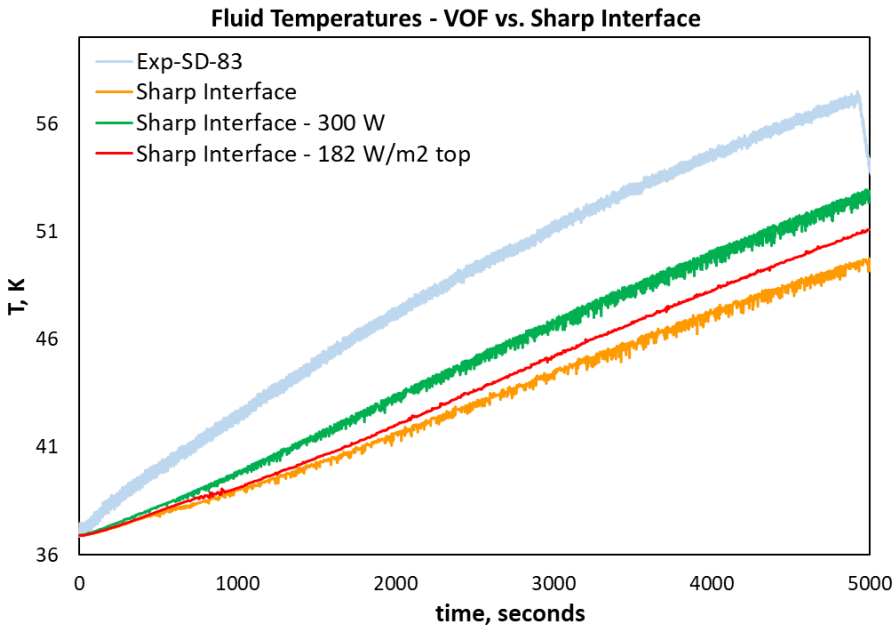

Figure 19: Effect of Tank Heat Load – Comparison of vapor temperatures at the SD-83 location

J. Heat Distribution in the Tank Predicted by the Sharp Interface Model

Heat distribution in the tank during self-pressurization predicted by the Laminar Sharp Interface model is analyzed in this section. This includes the analysis of the heat coming through that tank wall that is being distributed between the liquid and vapor regions and heat and mass transfer at the liquid-vapor interface. A schematic of heat distribution in the SHIIVER tank predicted by the Laminar Sharp Interface model is presented in Fig. 20. Here, positive directions are assumed to be for heat to go from the outside of the tank into the fluid through the tank wall and the direction of evaporation at the interface. The schematic shows that most of the heat is coming from the outside of the tank wall on the liquid side and staying in the liquid region. A smaller portion of heat is entering through the vapor side of the tank wall and a small portion of it is staying in the vapor region. In both liquid and vapor regions heat goes to the interface and the mass and energy balance at the interface results in total evaporation. The abbreviations here and on the following plots are as follows:

QWVO – Heat entering the tank from the outside on the vapor (dry) side of the wall

QWLO – Heat entering the tank from the outside on the liquid (wetted) side of the wall

QWLI – Heat entering Liquid region from the tank wall

QWVI – Heat entering Vapor region from the tank wall

QIV – Heat being transferred from the interface to the Vapor region

QIL – Heat being transferred from the Liquid region to the interface (positive sign is in the direction of evaporation or from Liquid to Vapor)

QTO – Total heat entering the tank at the outside wall

QTI – Total heat going into the fluid from the tank wall

m – interfacial mass transfer rate

L – Latent Heat

The plot shown in Fig. 21 shows evolutions of heat distribution at the interface. It shows that during self-pressurization of the SHIIVER tank the heat is supplied from both liquid and vapor to the interface resulting in evaporation at the interface. Evolutions of heat entering through the tank wall are presented in Fig. 22. Evolutions of heat entering through the outside of the tank wall (Boundary Conditions) separated between the liquid and vapor regions are plotted in Fig. 22-a. Total heat evolutions entering through the outside of the tank wall (Boundary Conditions) vs. coming into the fluid inside the tank are plotted in Fig. 22-b. The heat applied on the outside of the tank wall in the liquid region (wetted wall) is about double of the heat applied on the outside of the tank wall in the vapor region (due to 70% fill level). More than the amount of heat that applied on the outside of the wetted tank wall is pulled into the liquid region. This is due to the heat transferred inside the tank wall from the dry into the wetted portion of the wall. A small portion of heat entering the tank on the outside of the dry tank wall entering the vapor

region, some of this heat is conducted into the wetted wall and entering the liquid region and some of it goes to increasing the temperature of the tank wall. Fig. 23 shows the amount of heat remaining in the vapor region, calculated as: QWVI+QIV which is small compared to the heat entering the tank. It averages to 150-200 W.

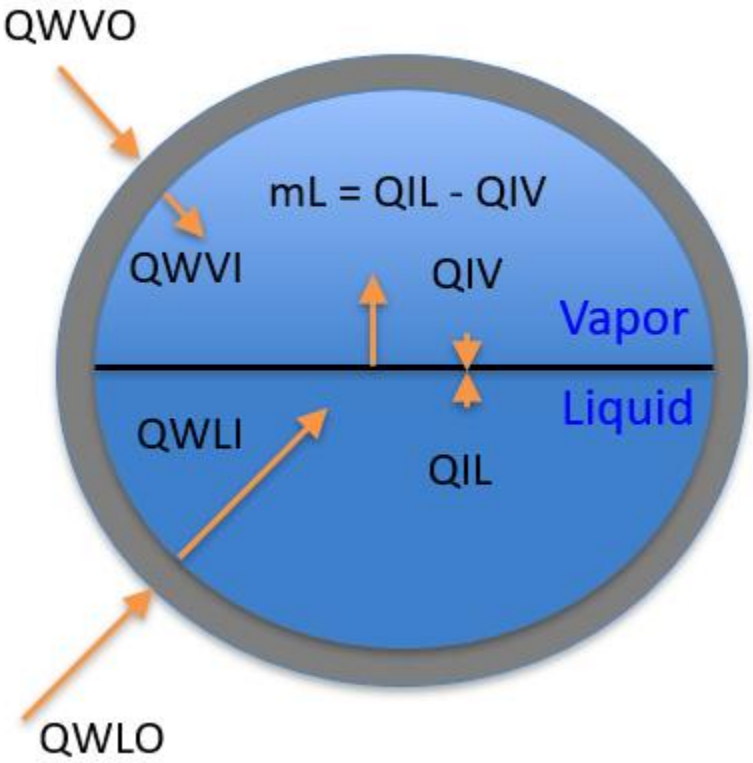

Figure 20: Schematic of heat distribution in the SHIIVER tank (Laminar model)

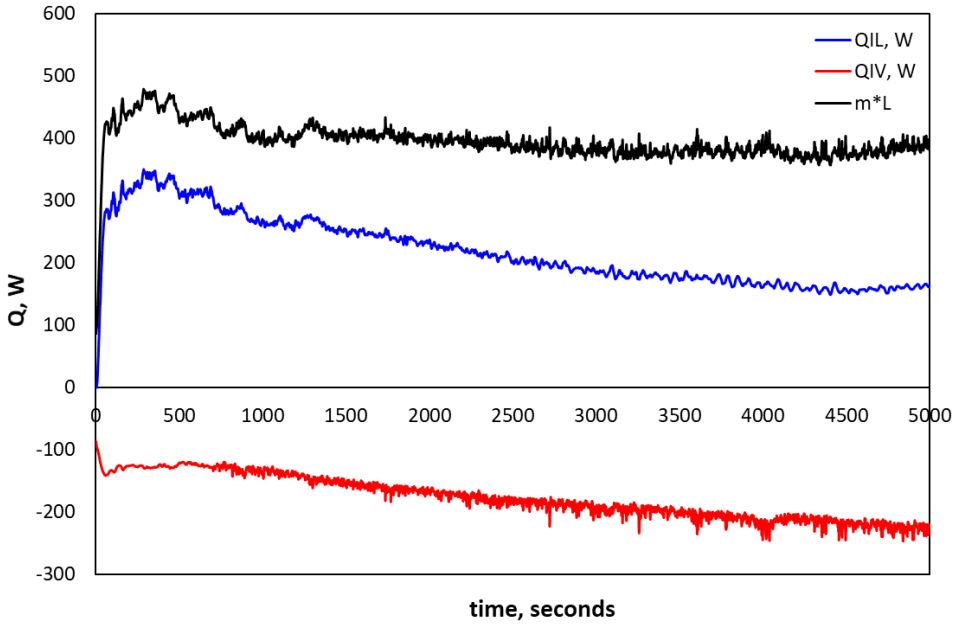

Figure 21: Evolutions of QIL, QIV and m_dot*L

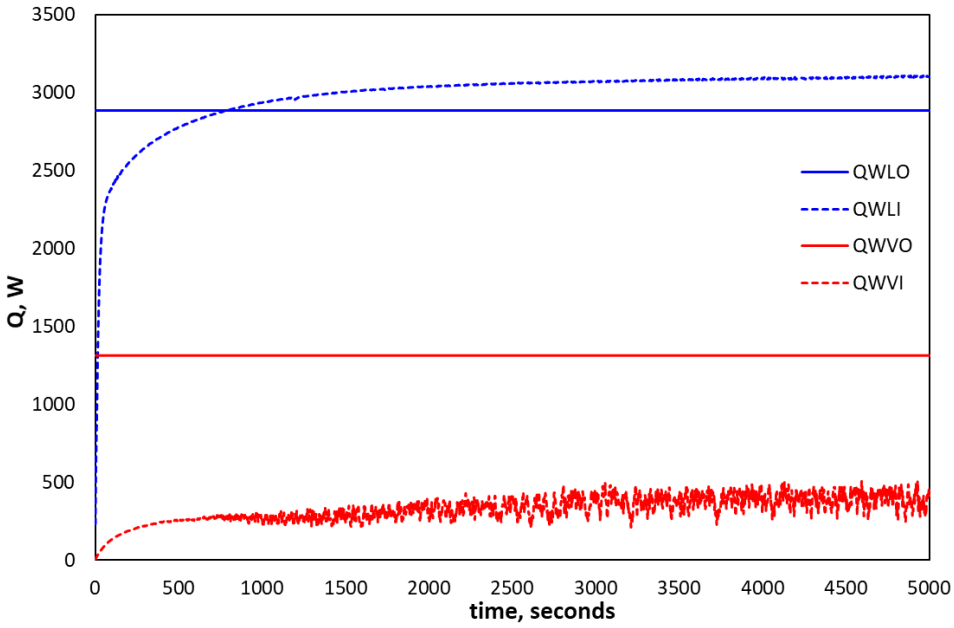

a) separated between the liquid and vapor regions

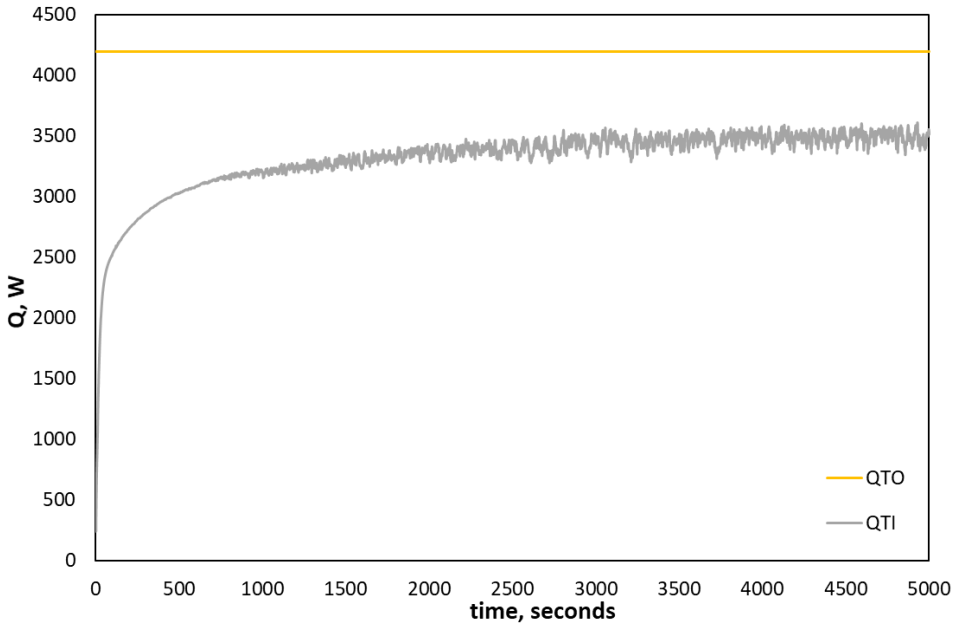

b) total

Figure 22: Evolutions of heat entering through the tank wall

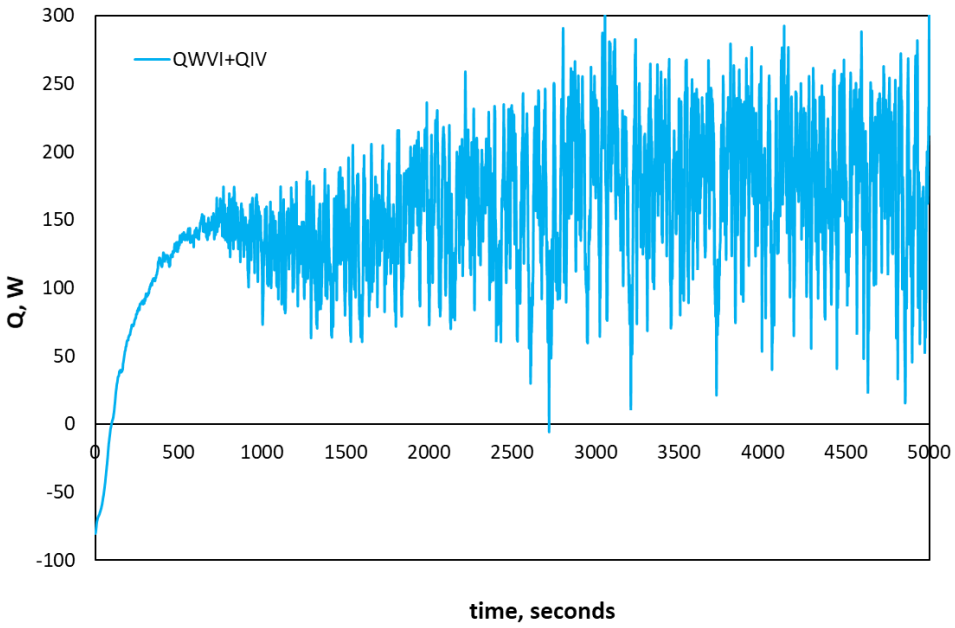

Figure 23: Amount of heat remaining in the vapor region

VII. Conclusion

Two-Phase flow and heat transfer simulations with interfacial phase change of the Structural Heat Intercept, Insulation, and Vibration Evaluation Rig (SHIIVER) self-pressurization case were conducted using in-house developed storage tank CFD model in the framework of the ANSYS Fluent CFD code. The simulations were performed for the 70% fill level case with MLI on domes and no vapor cooling. All the phase change calculations in these simulations were generated by a kinetic based evaporation-condensation model which was implemented through a customized Fluent UDF. The calculations were performed using both the VOF and Sharp Interface multiphase 2D axisymmetric models.

A number of parametric and sensitivity studies were performed to check the various aspects of the CFD model. These studies helped to understand the effects of varying several parameters on the tank pressure and temperature during self-pressurization. These parameters include: the effect of turbulence modeling and turbulence damping at the interface; the effect of constant vs. temperature dependent fluid properties; the effect of accommodation coefficient; and the effect of modeling phase change at the interface. The results of the VOF model were compared with the results of the Sharp Interface multiphase model. Despite the natural convection in a large tank being turbulent in nature, the Laminar model resulted in a more accurate prediction of the tank pressure and liquid temperatures compared to the experimental data. The Turbulent model significantly underpredicted experimental tank pressures and predicted vapor temperature decrease instead of increase observed in the experiment. This underlines the deficiency of existing Turbulence models, which overpredict the mixing in the vapor region and unrealistically enhance the heat transfer at the liquid-vapor interface when used with the VOF multiphase model, where continuity of turbulent quantities is applied at the interface. Even when a Turbulence model was used with the Sharp Interface multiphase model, where turbulent quantities are dampened at the interface, it resulted in a poorer agreement with the experimental data for tank pressures and temperatures compared to the results of the Laminar Sharp Interface Model. When the turbulence damping at the interface, available in the ANSYS Fluent CFD code was applied the results improved. However, the model with damping still underpredicted tank pressures and temperatures measured in the experiment and the ones predicted by the Laminar VOF model. Changing the accommodation coefficient used in the Schrage equation for the interfacial mass transfer rate calculation didn't affect the tank pressure and fluid temperature predictions, as it was expected for near-equilibrium tank conditions during self-pressurization. These results are, also, consistent with the results of varying accommodation coefficient in other large tank self-pressurization simulations.[9] Making fluid properties (specific heat, conductivity and viscosity) temperature dependent helped to significantly improve tank pressure predictions over a case with constant properties calculated at the initial saturation conditions.

The VOF and Sharp Interface multiphase models produced very similar results, both within 4% of the experimental tank pressure values.

Vapor temperatures were underpredicted in all CFD cases. Parametric tests were completed to study an effect of the heat load for the forward dome on the vapor temperature predictions. The results showed that increasing forward dome heat load increases vapor temperatures but doesn't have a significant effect on the tank pressure or interfacial mass transfer rate. This supports a theory that the forward dome heat load is possibly variable or affected by the tank hardware not included in CFD that conducted more heat into the top of the vapor region.

The results of this investigation effort showed that the current storage tank CFD model implemented in ANSYS Fluent CFD code is capable of predicting tank pressures during self-pressurization of a large tank in normal gravity within 4% of the measured values.

Acknowledgments

This work was supported by the NASA Space Technology Mission Directorate's Technology Demonstration Missions Program under the Evolvable Cryogenics Project.

References

[1] Johnson, W.L, Balasubramaniam, R., Hibbs, R.G., Zimmerli, G.A., Asipauskas, M., Bittinger, S.A., Dardano, C., and Koci, F.D. "Demonstration of Multilayer Insulation, Vapor Cooling of Structure, and Mass Gauging for Large-Scale Upper Stages: Structural Heat Intercept, Insulation, and Vibration Evaluation Rig (SHIIVER) Final Report", NASA/TP-20205008233, August 2021.

[2] Barsi, S. and Kassemi, M. "Investigation of Tank Pressurization and Pressure Control-Part II: Numerical Modelling", ASME Journal of Thermal Science & Engineering Applications, Vol. 5, No 2, pp- 041006: 1-9, December 2013

[3] Kartuzova, O., Kassemi M., "Modeling Interfacial Turbulent Heat Transfer during Ventless Pressurization of a Large Scale Cryogenic Storage Tank in Microgravity," *AIAA 47th Joint Propulsion Conference*, AIAA, San Diego, CA, 2011

[4] Grayson, G.D., Lopez, A., Chandler, F.O., Hastings L.J., Tucker, S.P., "Cryogenic Tank Modeling for the Saturn AS-203 Experiment," *Proceedings of the 42nd AIAA/ASME/SAE/ASEE Joint Propulsion Conference*, AIAA 2006-5258, 2006.

[5] Barsi, S., Kassemi, M., "Numerical and Experimental Comparisons of the Self-Pressurization Behavior of an LH2 Tank in Normal Gravity", *Cryogenics*, 48(3/4), pp. 122-129, 2007.

[6] M. Kassemi, S. Hylton, O. Kartuzova, "1G and Microgravity Tank Self-Pressurization: Experiments and CFD Model Validations across Ra and Bo Regimes", International Journal of Microgravity Science and Application, Vol 37, No.1, 2020, p. 370103-1.

[7] Kassemi, M., Kartuzova, O., Hylton, S. 2018, "Validation of two-phase CFD models for propellant tank self-pressurization: Crossing fluid types, scales, and gravity levels", Cryogenics, vol. 89, pp. 1-15

[8] Marek, R., and Straub, J., "Analysis of the evaporation coefficient and the condensation coefficient of water," *International Journal of Heat and Mass Transfer*, Vol. 44, 2001, pp. 39-53.

[9] O. Kartuzova, M. Kassemi "CFD Modeling of the Multipurpose Hydrogen Test Bed (MHTB) Self-Pressurization and Spray Bar Mixing Experiments in Normal Gravity: Effect of the Accommodation Coefficient on the Tank Pressure" 51st AIAA/ASME/SAE/ASEE Joint Propulsion Conference proceedings, July 2015, Orlando, FL, AIAA2015-3769

[10] C.W. Hirt and B.D. Nichols, "*Volume of fluid (VOF) method for the dynamics of free boundaries*", *Journal of Computational Physics* **39** (1): 201-225. 1981.

[11] R.W. Schrage, A theoretical study of interphase mass transfer, Columbia University Press, New York, 1953.

[12] Brackbill J.U., Kothe, D.B., Zemach, C., "A continuum method for modeling surface tension," J. Comp. Phys. Vol. 100, 1992, pp. 335–354.

[13] Menter, F. R., "Two-Equation Eddy-Viscosity Turbulence Models for Engineering Applications," AIAA Journal, 32(8), 1994, pp. 1598-1605.

[14] Wilcox, D.C., *Turbulent Modeling for CFD*, DCW Industries, Inc., La Canada, California, 1998.